UDC 621.382.2

E. F. Venger[1], A. I. Ievtushenko[2], L. Yu. Melnichuk[2], O. V. Melnichuk[2]
[1] Institute of Semiconductor Physics V. Lashkarev NAS Ukraine, Kyiv, Ukraine
[2] Nizhyn Gogol State University, Nizhyn, Ukraine

THE INVESTIGATION OF SURFACE EXCITATIONS IN OPTICALLY-ANISOTROPIC ZnO SINGLE CRYSTALS PLACED IN A UNIFORM MAGNETIC FIELD

With the help of external reflection spectroscopy (EF) and attenuated total reflection (ATR) the investigation of optical and electrophysical properties of polar uniaxial optically-anisotropic ZnO single crystal placed in a uniform magnetic field (Faraday and Voigt configurations) was conducted. The area of display of new oscillations caused by the influence of a uniform magnetic field was detected for the first time in the spectra of external IR-reflection of ZnO single crystal and the interaction of phonons with plasmons under the same conditions was investigated. The influence of the magnetic field on the basic properties of surface polaritons (SP) according to orientations $C\Pi x$, $\vec{k}\Pi C$, $xy\Pi C$; $C\Pi y$, $\vec{k} \perp C$, $xy\Pi C$; $C\Pi z$, $\vec{k} \perp C$, $xy \perp C$ was revealed.

Introduction. Despite many years of research, uniaxial polar single crystals remain the subject of active research of modernity since they are widely used in various fields of science, technology, medicine, etc. [1], [2], [3], [4]. Particularly, ZnO is a potential material for Photonics, Spintronics and Nanoelectronics [1], [5], [3], [7], [8], [9], [10]. In addition, ZnO is effective while creating UV LEDs, solar-blind photodetectors (UV-detectors) and gas sensors [8], [9], [10]. The advantage of ZnO the over other materials is its transparency to visible radiation and high thermal and chemical stability [8], [9].

ZnO is characterised by the significant anisotropy of phonon subsystem properties and by the weak anisotropy of plasma subsystem. It is a binary compound of A^2B^6 type [1], [3]. Its structure is presented in Fig. 1. Under normal conditions macroscopic ZnO crystallizes only in the wurtzite structure, which turns into NaCl structure under hydrostatic compression (~ 8 GPa). Through heteroepitaxial growth it is possible to grow ZnO in the structure of sphalerite on substrates with cubic structure, which can be implemented for a number of morphological nanostructures [11]. ZnO is a uniaxial crystal with a band gap $E_{cv} \leq 3,43$ eB and *n*-type of conductance [12].

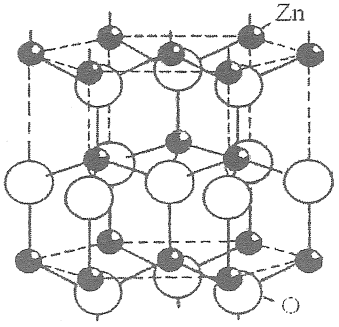

Fig. 1 — ZnO structure [1]

Despite various publications, the characteristic of "non-magnetic" solids exposed to magnetic fields, the typical representative of which is ZnO, is still under study [1], [13]. Its influence on some properties of non-magnetic crystals, including ductility, was experimentally recorded [14], [15], [16].

Experimental research in ZnO single crystals reflection coefficients and light absorption at low temperatures in magnetic fields has been conducted [1]. The authors [17] described the experimental data obtained in the light propagation parallel to axis of symmetry; therefore, there is no need to take into account birefringence under these conditions. The experiments on Faraday's rotation on ZnO materials with uniaxial symmetry were conducted in the article [18].

Some interesting results were received [19], [20], [21], they show that under the condition of ZnO doped by Sc, Ti, V, Cr, Mn, Fe, Co, Ni, Cu, it changes not only its type of con-

ductivity but also some magnetic properties manifestation. Thus, in thin ZnO films, doped with cobalt, ferromagnetism at room temperature was detected.

It is clear that the usage of polar uniaxial optically-anisotropic ZnO semiconductors and films based on them in order to create a number of semiconductor devices, which are capable to work under the influence of strong magnetic fields, of course, requires the investigation of the magnetic field influence on their optical and electrophysical properties.

Optical methods are the most effective among non-destructive methods, which allow to control the quality and structural perfection of the crystals; and to investigate the condition of their surface. IR-spectroscopy method can provide information on the molecular (atomic) structure and on the symmetry of internal stresses of a solid. This method is used [5] to investigate IR dielectric function and phonon catching for ZnO films. The spectra of ZnO nanocrystals, grown by pulsed laser deposition on sapphire and silicon were described in the article [5].

The authors of the article researched the spectra of external reflection from the surface of ZnO with the concentration of electrons from 10^{16} to $5 \cdot 10^{19}$ cm^{-3}. The mutually consistent bulk parameters of zinc oxide single crystals were obtained and presented in Table 1, 2. ZnO single crystals, grown with the help of hydrothermal synthesis method, were used. ZnO samples were rectangular parallelepipeds $10 \times 8 \times 8$ mm^3 with faces, the two of which are perpendicular to the axis *C*.

Venger E. F. alongside with the other scientists [3], [22] investigated the reflection coefficient of ZnO single crystals in the IR-spectrum, considering oscillations of three pairs of interacting subsystems: electromagnetic waves, optical oscillations of the grid and plasma oscillations of free charge carriers for orientations $E \perp C$ and $E \| C$. It was the first attempt in this field.

Methods of research. The measurement of IR-reflection spectra from the surface of ZnO single crystal was carried out in the range of wavenumbers from 200 to 4 000 cm^{-1} on a spectrophotometer SPECORD-M80, which works according to two-beam scheme.

The degree of polarization of IR-radiation is 98%.

Experimental IR-reflectance spectra in the magnetic field from the surface of ZnO single crystals were obtained in the frequency range 550...1 400 cm^{-1} using Fourier's IR-spectrometer Infralum FT-801, which works according to one-beam optical scheme.

In Fig. 2 the scheme of experimental installation is presented. The sample was placed between the poles of the electromagnet into a special holder. The Angle of IR-radiation incidence on the edge of the sample was 18°.

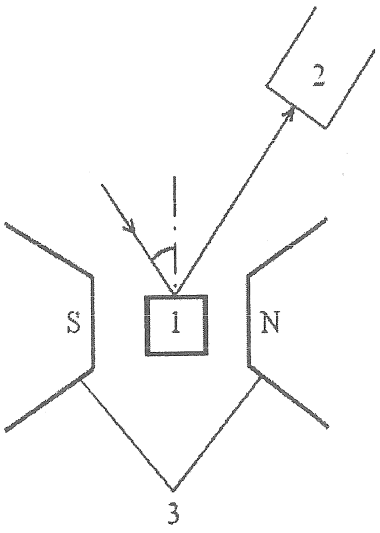

Fig. 2 — *1* — Sample, *2* — IR-photodetector of Infralum FT-801 spectrometer, *3* — Poles of the magnet

All the measurements were carried out at room temperature and in the magnetic field up to 22 kOe, generated by the electromagnet. The reflection coefficient $R(\nu)$ was determined with an accuracy of 1...2%. The resolution was within a specified range of 1 cm^{-1}.

For the investigation of phonon and plasmon-phonon polaritons spectrometer ИКС-29М and ATR attachment НПВО-2 were used [3]. The device operates when the range varies from 380 to 4 200 cm^{-1}. The range of angles of

light incidence on the element ATR varies from 20° up to 60° with the precision of installation of angles not less than 6'. The interval between half-cylinders and crystals is created by means of calibrated PTFE gaskets.

Results and Discussion. The investigation of IR-reflection spectra and attenuated total reflection (ATR) in uniaxial optically anisotropic crystals ZnO, placed in a uniform magnetic field, was conducted with the following configurations:

I. Faraday Configuration (magnetic field and direction of propagation of light wave $\vec{k}$ is directed along the normal to the surface of the crystal):

I*a* — Optical axis of the crystal is parallel to the magnetic field;

I*b* — Optical axis of the crystal is perpendicular to the magnetic field;

Voigt Configuration (electromagnetic wave propagates in uniaxial semiconductor perpendicular to the optical axis of the crystal and uniform magnetic field $\vec{H}$): II*a* — Axis of the crystal is perpendicular to the reflecting surface in orientation $\vec{E}_0 \text{II} \vec{H}$;

II*b* — Axis of the crystal is perpendicular to the reflecting surface in orientation $\vec{E}_0 \perp \vec{H}$;

II*c* — Axis of the crystal is parallel to the reflecting surface in orientation $\vec{E}_0 \text{II} \vec{H}$;

II*d* — Axis of the crystal is parallel to the reflecting surface in orientation $\vec{E}_0 \perp \vec{H}$;

II*e* — Axis of the crystal is parallel to the reflecting surface in orientation $\vec{E}_0 \text{II} \vec{H}$ and *C*;

II*f* — Axis of the crystal is parallel to the reflecting surface in orientations $\vec{E}_0 \perp \vec{H}$ and *C*, and $\vec{H} \text{II} C$.

Figs. 3—6 show the theoretical and experimental spectra of IR-reflection of ZnO single crystal with optical and electrophysical parameters (Tables 1, 2). The mathematical model, by means of which the calculation was carried out, is described in many works [23], [24], [25]. Curve 1 (*see* Figs. 3—6) corresponds to the dependency $R(\nu)$ in case of the absence of the magnetic field influence on the sample. It is coordinated with the experimentally obtained curve $R(\nu)$ in the monograph [3] for the monooscillator ZnO model (points in Fig. 3). Curves 2—4 (*see* Fig. 3) correspond to dependencies $R(\nu)$ in the case of the presence of a uniform magnetic field in the range of 30...100 kOe.

Fig. 3 shows, that under the influence of a uniform magnetic field (in cases I*a*, *b*, II*b*, *d*,*e*) the number of the minimum and maximum points of the reflection coefficient increase and their shift to the high-frequency range with the increase of magnetic field takes place. In Table 3 the frequencies of minimum ν_{min} and maximum ν_{max} of reflection spectra are shown depending on the magnitude and direction of the magnetic field, relative to the optical axis and semiconductor surface that was investigated. These data are consistent with the experimental studies described in the study by Tsydilkovs'ky [26] where it is shown that, in case of propagation of unpolarized light along a magnetic field, the wave electric vector is always perpendicular to the field and can be decomposed into two circularly polarized components with opposite rotation direction. If spread in the direction perpendicular to the direction of the magnetic field, unpolarized light can be decomposed into two linearly polarized parallel and perpendicular to the field components. The last component leads to the splitting of minimum in reflection spectra.

Fig. 4. presents reflection spectra $R(\nu)$ of the sample ZO6-B in the case II*e*. For other orientations spectra differ only in frequency bands in which the influence of magnetic field on the single crystal appears. In cases I*a* the influence of magnetic field on ZnO single crystal is observed by IR-reflection spectra in the frequency range 0...380 cm^{-1}, I*b* — 0...360 cm^{-1}, II*b* — 0...380 cm^{-1}, II*d* — 0...360 cm^{-1}, II*f* — 0...370 cm^{-1} and less in ranges I*a* — 710...890 cm^{-1}, I*b* — 730...900 cm^{-1}, II*b* — 630...910 cm^{-1}, II*d* — 620...940 cm^{-1}, II*f* — 640...840 cm^{-1}. Consequently, apart from the influence of anisotropy of phonon and plasma subsystems of ZnO single crystal according to spectra of external IR-reflection effect of anisotropy, caused by a magnetic field, is observed.

Asitis shown in Fig. 4, the influence of a uniform magnetic field can not be detected by reflection spectra in the frequency range. However, in the range from 250 to 380 cm^{-1} the maximum change of external reflection

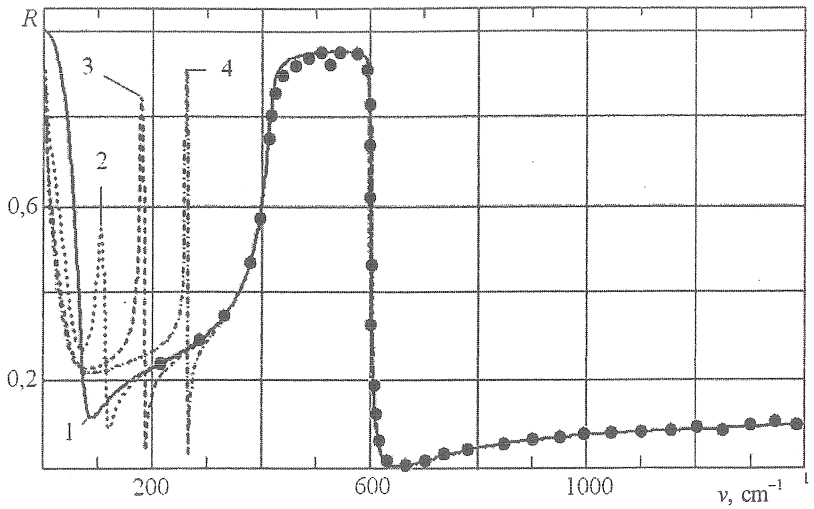

Fig. 3 — Reflection $R(\nu)$ of ZO2-3 single crystal placed in a uniform magnetic field: *1* — H = 1E; *2* — H = 30 kOe; *3* — H = 65 kOe; *4* — H = 100 kOe

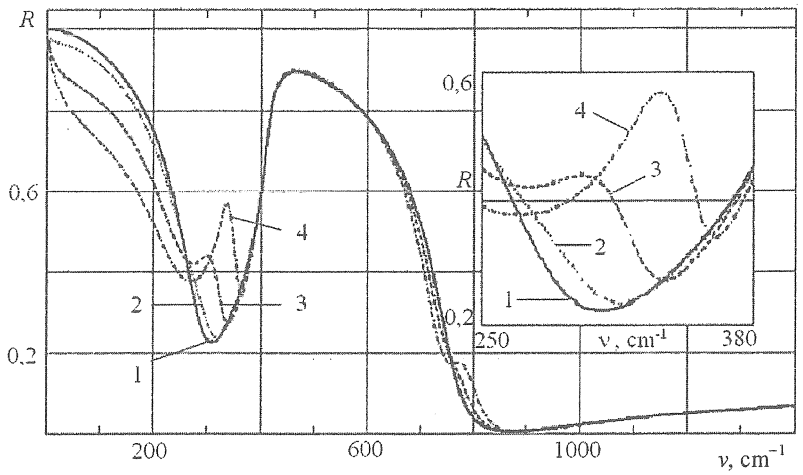

Fig. 4 — Reflection spectra $R(\nu)$ of ZO6-B single crystal placed in a uniform magnetic field: *1* — H = 1E; *2* — H = 30 kOe; *3* — H = 65 kOe; *4* — H = 100 kOe. In the insert — dependence $R(\nu)$ in the frequency range from 250 to 380 cm^{-1}

coefficient of heavily doped single crystal is observed, this change is caused by the influence of the uniform magnetic field on ZnO sample (Fig. 4). In contrast to the previous case, the manifestation of new maximums and minimums in case of increase of magnetic field in the range ≈ 300 cm^{-1} was registered in IR-spectra of external reflection. However, as it is shown by means of mathematical experiment, their amplitude and shift to the high-frequency IR-area in case of growing magnetic field are insignificant, while impurities in semiconductors lead to increase of Landau levels [27].

Under these conditions strong magnetic fields are required for satisfactory separation of levels.

Figs. 5 and 6 show the dependencies $R(\nu)$ for undoped ZnO single crystals for different values of phonon attenuation coefficient, constant plasma frequency and plasmon attenuation coefficient in a magnetic field of 65 kOe.

As it is shown in Fig. 5, in case of $\nu_p = \gamma_p =$ = 100 cm^{-1}, one more maximum and minimum

Table 1 — Bulk parameters of ZnO [3], [22]

ZnO	ε_0	ε_∞	ν_T, cm^{-1}	ν_L, cm^{-1}
$E \perp C$	8,10	3,95	412	591
$E \parallel C$	9,00	4,05	380	570

Table 2 — Electrophysical parameters of ZnO single crystals, grown by hydrothermal method [3], [22]

№	Sample	n_0, cm^{-3}	ν_p, cm^{-1}		γ_p, cm^{-1}		γ_f cm^{-1}		m_{II}	$\frac{m_\perp}{m_{II}}$	$m_\perp$	μ_{II}	$\mu_\perp$
			$E \perp C$	$E \parallel C$	$E \perp C$	$E \parallel C$	$E \perp C$	$E \parallel C$					
1	ZO2-3	$9{,}3 \cdot 10^{16}$	90	100	150	170	11	11	0,21	1,23	0,258	4,76	3,88
2	ZO1-3	$6{,}6 \cdot 10^{17}$	240	250	280	260	13	13	0,23	1,13	0,260	4,35	3,85
3	ZO6-B	$2{,}0 \cdot 10^{18}$	420	480	406	350	21	21	0,22	1,18	0,260	4,55	3,85

Table 3 — Minima and maxima frequencies of reflection spectra of undoped ZnO single crystal in a magnetic field

Frequencies	ν_{min}, cm^{-1}					ν_{max}, cm^{-1}				
Configurations / *H*, kOe	I*a*	I*b*	II*b*	II*d*	II*f*	I*a*	I*b*	II*b*	II*d*	II*f*
10^{-3}	82	83	82	79	89	—	—	—	—	—
30	114	119	118	118	115	69	76	104	103	98
65	173	187	186	186	172	148	164	177	177	163
100	242	264	264	264	242	228	252	259	259	236

appear in a uniform magnetic field of 65 kOe at frequencies 180 and 190 cm^{-1}, they do not change the intensity with the change of phonon attenuation in the reflection spectrum. Phonon attenuation manifests in the range $R(\nu)$ from 390 to 600 cm^{-1} through the decrease of reflection intensity in case of the phonon attenuation coefficient increase.

Fig. 6 shows the reflection spectra of ZnO single crystal with plasma frequency $\nu_p = 500$ cm^{-1} and plasmon attenuation coefficient $\gamma_p = 500$ cm^{-1}. It is clear that in the range 250...380 cm^{-1} (insert in Fig. 6) $R_{min}(\nu)$ increases from 0,29 up to 0,36 with phonon attenuation coefficient γ_f increase from 11 to 30 cm^{-1}. At the same time, the decrease $R_{max}(\nu)$ from 0,92 to 0,87 cm^{-1} in the range 400...570 cm^{-1} is observed.

Analyzing external reflection spectra (*see* Figs. 3—6) we can conclude that the strongest influence of a uniform magnetic field on the reflection coefficient of ZnO single crystal surface was caused by the undoped semiconductor.

Figs. 7—8 present the dependency of reflection coefficient from the value of a uniform magnetic field respectively on minimum and maximum frequencies for undoped ZnO single crystal (sample ZO2-3). This can be seen in Fig. 3 (Curves 2—4).

All the calculations indicate a linear character of the frequency dependency, where the additional minimum of the magnetic field is observed (Table 3). The chart in Fig. 9 shows the dependency of minima frequencies in magnetoabsorption spectra from magnetic field: 1 — case II*b*, 2 — II*f*. It is to be noted, the equivalent will be the dependency of additional maxima frequencies in magnetoabsorption spectra from the strength of magnetic field.

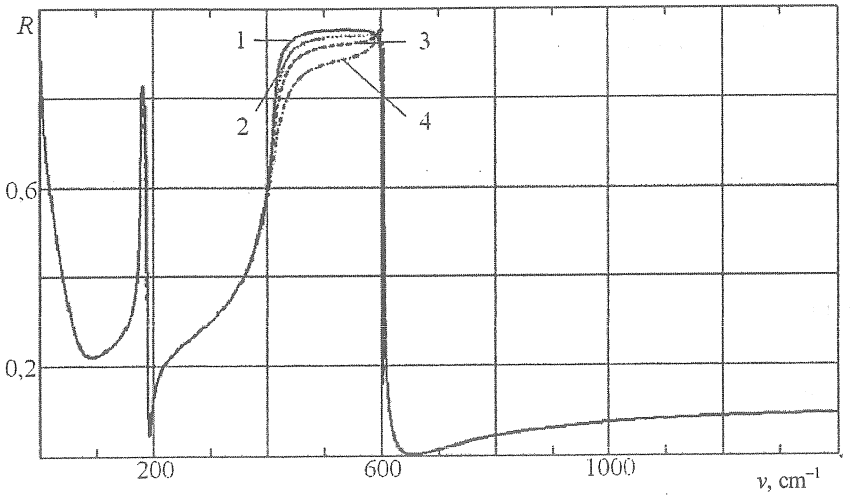

Fig. 5 — Dependency $R(\nu)$ of ZnO single crystal ($\nu_p = \gamma_p = 100$ cm^{-1}, $H = 65$ kOe): *1* — $\gamma_f = 11$ cm^{-1}; *2* — $\gamma_f = 15$ cm^{-1}; *3* — $\gamma_f = 20$ cm^{-1}; *4* — $\gamma_f = 30$ cm^{-1}

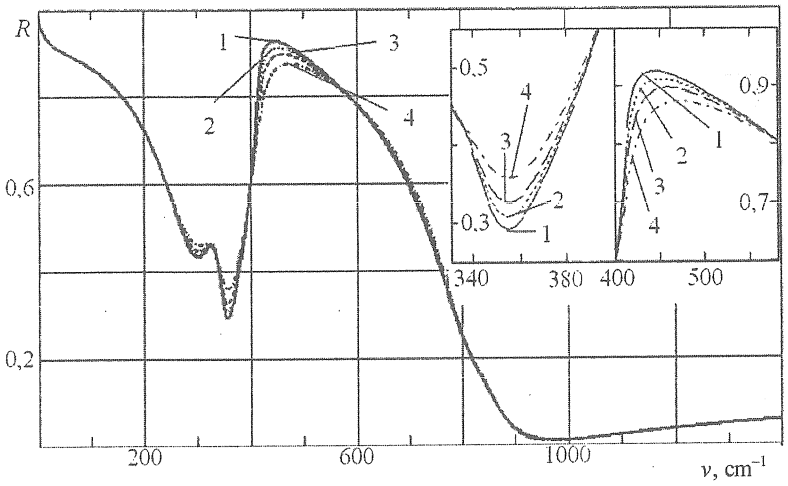

Fig. 6 — Dependency $R(\nu)$ of ZnO single crystal ($\nu_p = \gamma_p = 500$ cm $H = 65$ kOe): *1* — $\gamma_f = 11$ cm^{-1}; *2* — $\gamma_f = 15$ cm^{-1}; *3* — $\gamma_f = 20$ cm^{-1}; *4* — $\gamma_f = 30$ cm^{-1}

The manifestation of magneto-refractive effect in polar optically-anisotropic ZnO single crystals and its dependence from the magnitude and direction of the magnetic field, concentrations of free charge carriers and attenuation coefficients of phonon and plasmon are investigated in the article as well [28].

Fig. 10 shows the calculated spectra of magnetoreflectance $\Delta R/R$ from the surface of ZnO, subjected to the influence of the uniform magnetic field of 30 kOe (orientation II*e*). As seen from Fig. 10, the value for ZnO is $\Delta R/R \approx 3\%$ specified by the magnetic field.

Fig. 11 presents magnetoreflectance $\Delta R/R$ spectra of ZnO single crystal with different values of external magnetic fields. In contrast to magnetoreflectance spectra for 6H-SiC single crystals, heavily doped ZnO (Fig. 12) and dielectrics [29], changes of spectral position of minima $\Delta R/R$ subjected to different magnetic fields are observed in the undoped semiconductor ZnO. As seen in Fig.11, spectra of magnetoreflectance of undoped ZnO have minima at frequencies $\nu = 98$; 163; 236 cm^{-1} (*see* Table 3), which correspond to the frequency of additional maxima in

ZnO reflection spectra in case of influence of magnetic fields on a single crystal (configuration II*f*).

Figs. 11, 12 show that the changes in the magnetoreflectance spectra can be observed in "residual rays" area of ZnO. Moreover, in case of free concentration increase charge carriers, decreases the coefficient of magnetore-flectance, and vice versa. In ZnO single crystals a sharp change of the effect in case of a little increase of the magnetic field is detected. Calculations show the dependency of magnetoreflectance coefficient from the concentration of free charge carriers and the value of external uniform magnetic field.

Fig. 13 shows the spectrum $\Delta R / R$ (points) of undoped ZnO in the range 580...700 cm^{-1}, obtained with the help of Infralum FT-801 spectrometer subjected to external magnetic field of 22 kOe (*see* Fig. 2), the line is the rated spectrum of magnetoreflectance. Judging by the experiment, the deflection of magnetoreflectance spectrum from zero within 7...12% is observed. In the case of the frequencies usage higher than 670 cm^{-1} $\Delta R / R = 0$, the coincidence of theoretical and experimental curves up to the experiment is observed.

The investigation of the dependence of magnetoreflectance coefficient (*see* Figs. 11, 12) from phonon and plasmon attenuation coefficient for ZnO single crystals was conducted for various concentrations of free charge carriers and uniform magnetic field. The mathematical model [30] was used. The results are presented in Table 4.

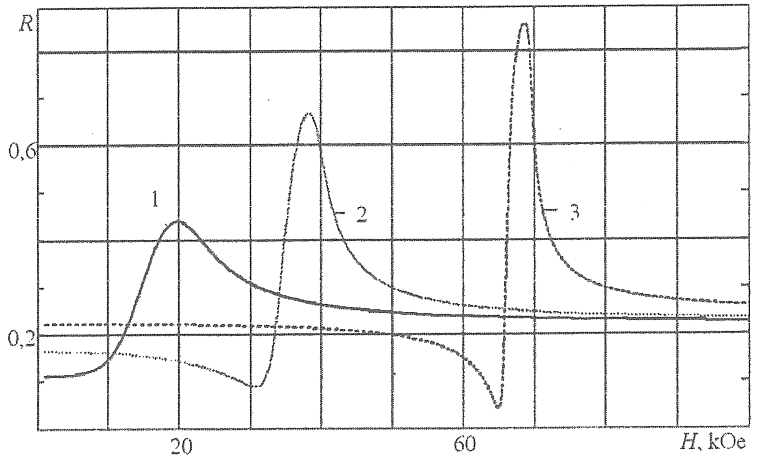

Fig. 7 — Dependency *R*(*H*) of ZnO single crystals (sample ZO2-3) in the frequency range of minima reflection spectra: *1* — $\nu = 88$ cm^{-1}; *2* — $\nu = 119$ cm^{-1}; *3* — $\nu = 186$ cm^{-1}

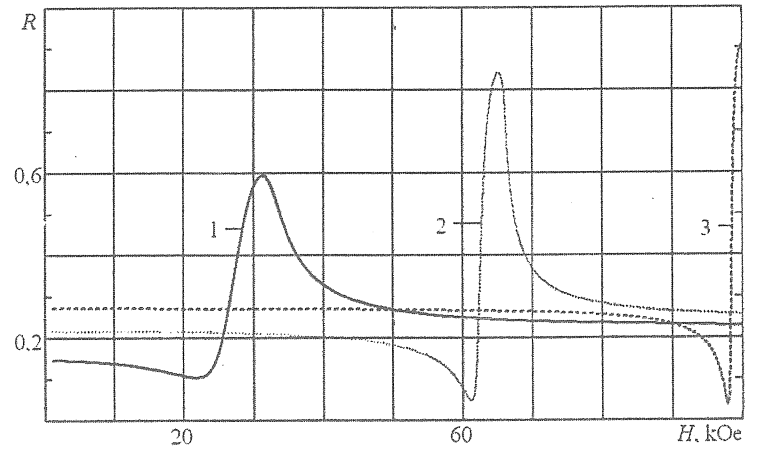

Fig. 8 — Dependency *R*(*H*) of ZnO single crystals (sample ZO2-3) in the frequency range of maxima reflection spectra: *1* — $\nu = 104$ cm^{-1}; *2* — $\nu = 177$ cm^{-1}; *3* — $\nu = 259$ cm^{-1}

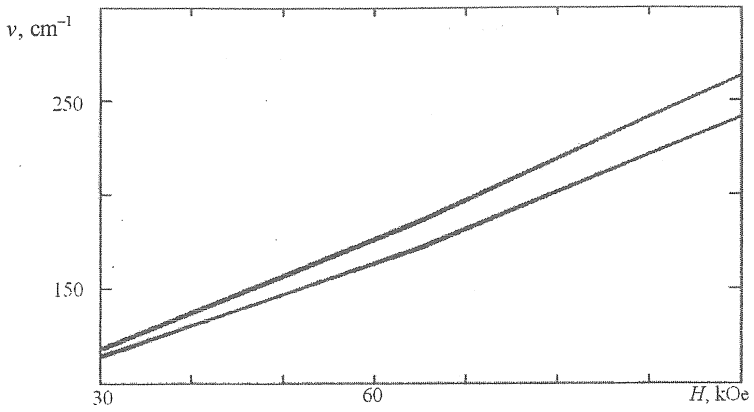

Fig. 9 — Fan pattern of ZnO crystal

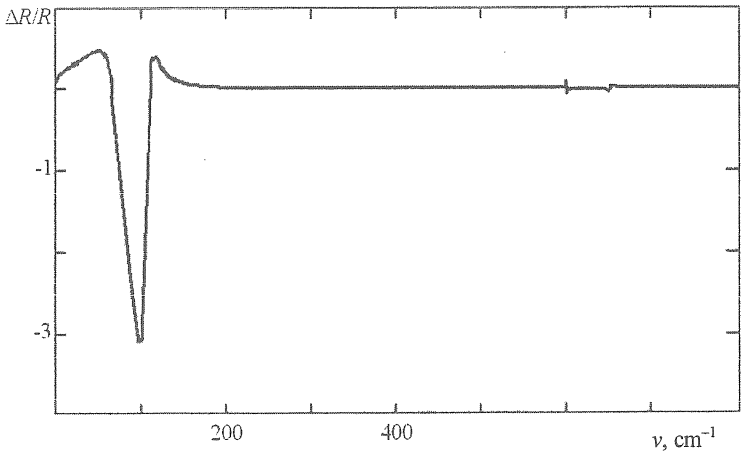

Fig. 10 — $\Delta R/R$ spectrum of ZnO single crystal, placed in the magnetic field of 30 kOe

According to the data presented in Table 4, the coefficient of magnetoreflectance is sensitive to changes in phonon γ_f and plasmon γ_p attenuation coefficients. Thus, with the increase of γ_f in heavily doped ZnO, the increase of $\Delta R/R$ in the range of high frequencies and the decrease in the range of low frequencies are detected. At the same time the increase of $\Delta R/R$ in the area of "residual rays" is registered with the increase of γ_p in the undoped ZnO. The increase of the concentration of electrons in ZnO is accompanied by the decrease of $\Delta R/R$.

Fig. 14 presents reflection spectra $R(v)$ of ZnO single crystals with different concentrations of free charge carriers under the influence of magnetic field of 50 kOe. As shown in Fig.14 there are no changes in the reflection spectra in heavily doped semiconductors $n_0 \approx 10^{18}$ cm^{-3} (curve 3). Calculations show that with the concentration of free charge carriers in ZnO $\leq 10^{17}$ cm^{-3} and with the magnetic field less than 30 kOe, no additional oscillations in the spectra $R(v)$ are observed.

It is well known, that the minimum $R(v)$ on the surface of optically anisotropic semiconductors placed in a magnetic field shifts to the value $\pm\Omega/2$ [26]. This is due to the fact that if the semiconductor is placed in a magnetic field, the movement of electrons in a circle with angular frequency

$$\Omega = \frac{eB}{mc}\sqrt{\mu_{\perp}\mu_{xx}} \qquad (1)$$

appears in the plain that is perpendicular to the field, and it is called cyclotron.

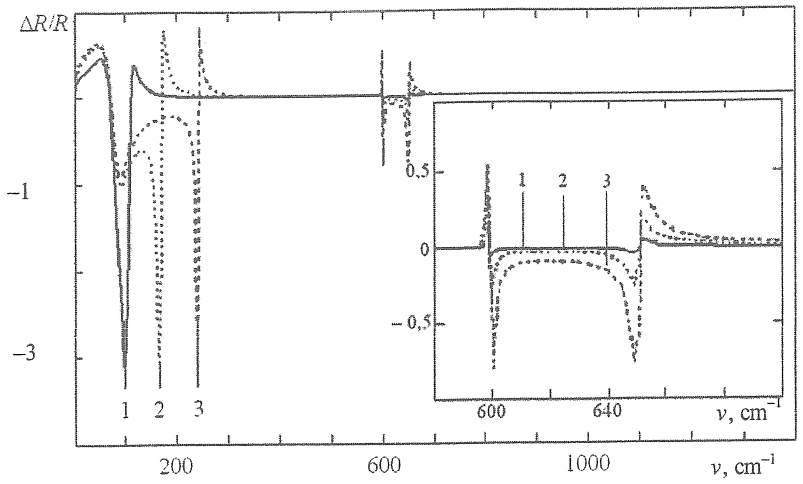

Fig. 11 — $\Delta R/R$ spectra of undoped ZnO single crystal with external magnetic field values of *1* — 30 kOe; *2* — 65 kOe; *3* — 100 kOe

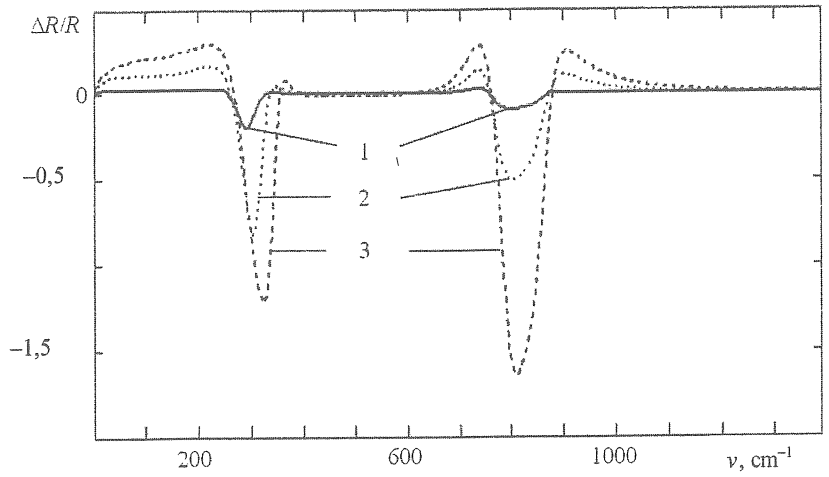

Fig. 12 — $\Delta R/R$ spectra of heavily doped ZnO with external magnetic field values of *1* — 30 kOe; *2* — 65 kOe; *3* — 100 kOe

The obtained orbits are quantized, so the states that correspond to different energies are concentrated into discrete subzones. The transitions between the latter will cause the appearance of peaks in the reflection spectrum [27]. And magnetic field will shift the bottom of the conduction band up, and the top of the valence band towards lower energies. Therefore, the experimental determination of the distances between minima in the spectra $R(\nu)$ makes it possible to fix Ω.

Table 5 shows the difference in frequency between the minima of ZnO reflection spectrum in the case of the single crystal external magnetic field influence and its absence. The data from Fig. 3 and the values of cyclotron frequency, defined by the formula (1) for the specified fields, were used. It is obvious that the minimum of reflective capacity shifts the value $\pm\Omega/2$ for fields not exceeding 30 kOe. This pattern is not observed for stronger external magnetic fields.

Table 6 presents the difference between the frequency of plasmons (Fig. 3) and the value of cyclotron frequency for ZnO single crystal, calculated with the help of the formula (1) with values of the magnetic field given in the legends in Fig. 3.

It is shown in table 6 the distance between the plasma edges is equal to cyclotron frequency only under the influence of fields of about 100 kOe. This equality is not satisfied with fields less than 100 kOe.

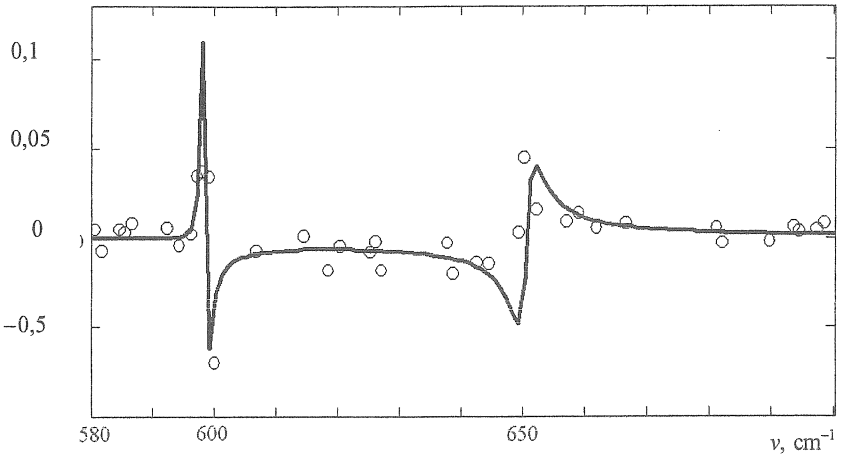

Fig. 13 — $\Delta R/R$ ZnO of 22 kOe: line — calculation; points — experiment

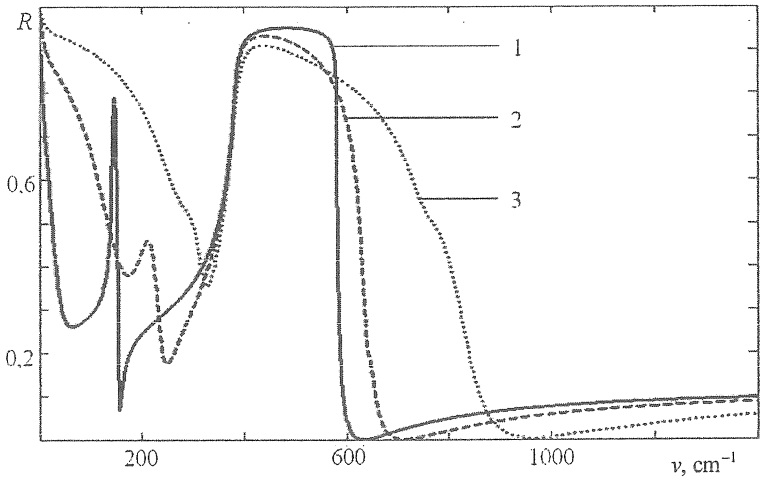

Fig. 14 — R (ν) of ZnO single crystals placed in a magnetic field of 50 kOe: 1 — ZO2-3 (n_0=9,3·10^{16} cm^{-3});

Many crystalline materials are characterized by the selective reflection at some wavelengths due to the increase of reflection coefficient in the narrow spectral range (from about 5 to 90%) [31]. This phenomenon occurs at a frequency higher than the frequency of the vibration motion of ions in the crystal lattice. This selective reflection provides afiltering effect. Analyzing ZnO reflection spectra, presented in Fig. 3 in magnetic fields of 30, 65, 10 kOe, we can see, that there are some additional areas of selective reflection (Table 7) in the reflection spectra. Fig. 3 and Fig. 7 show that the bands of selective reflection do not match in various magnetic fields. With the increase of magnetic field the shift of selective reflection is observed and the larger the magnetic field is, the better this shift is observed.

Using the data of IR-reflectance spectroscopy for optically anisotropic zinc oxide, the properties of surface polaritons specified single crystals were investigated.

Fig. 15, *a*, presents the calculated spectra of ATR I / I_0 of undoped zinc oxide (n_0 = 9,3 × × 10^{16} cm^{-3}), obtained with the help of the method, described [32], [33], [34] with orientation *C*II*x* (curve 1), *C*II*y* (curve 2), *C*II*z* (curve 3), recorded by the air gap d = 14,6 (1, 1′); 8,7 (2, 2′); 4,1 (3, 3′) mm and angles of 30° (1, 1′), 35° (2, 2′), 50° (3, 3′).

Table 4 — Minimums of ZnO magnetoreflectance and their dependence from γ_f and γ_p

ZnO	ZnO (ZO2-3, $n_0 = 9{,}3 \cdot 10^{16}$ cm^{-3})					
H, kOe	30		65		100	
γ_f, cm^{-1}	11	30	11	30	11	30
$\Delta R/R$	–3,1021	–2,9423	–3,0471	–2,825	–2,5847	–2,296
ν_{min1}, cm^{-1}	97		163		236	
γ_p, cm^{-1}	110	500	110	500	110	500
$\Delta R/R$	–3,1021	–5,6367	–3,0471	–3,0356	–2,5847	–2,4937
ν_{min1}, cm^{-1}	97	69	163	162	236	236
γ_f, cm^{-1}	11	30	11	30	11	30
$\Delta R/R$	—	—	—	—	—	—
ν_{min2}, cm^{-1}	—		—		—	
γ_p, cm^{-1}	110	500	110	500	110	500
$\Delta R/R$	—	—	—	—	—	—
ν_{min2}, cm^{-1}	—	—	—	—	—	—
ZnO	ZnO (ZO6-B, $n_0 = 2{,}0 \cdot 10^{18}$ cm^{-3})					
H, kOe	30		65		100	
γ_f, cm^{-1}	11	30	11	30	11	30
$\Delta R/R$	–0,2309	–0,1605	–1,0075	–0,6906	–1,4159	–1,0507
ν_{min1}, cm^{-1}	290	289	302	300	323	320
γ_p, cm^{-1}	110	500	110	500	110	500
$\Delta R/R$	–0,2325	–0,2407	–1,0387	–0,971	–1,2989	–1,2772
ν_{min1}, cm^{-1}	316	283	323	297	334	319
γ_f, cm^{-1}	11	30	11	30	11	30
$\Delta R/R$	–0,0821	–0,0983	–0,4472	–0,5563	–1,4203	–1,8711
ν_{min2}, cm^{-1}	797	793	801	798	808	806...807
γ_p, cm^{-1}	110	500	110	500	110	500
$\Delta R/R$	—	–0,0817	—	–0,4502	—	–1,432
ν_{min2}, cm^{-1}	—	791	—	794	—	801

The points are the experimental data for sample ZO2-3 [3]. The space of the air gap between the ATR prism and the sample ZO2-3 varied till the definition of the intensity of absorbed wave that does not exceed 20% at constant frequency minimum in the spectrum ATR [35]. Curves 1′, 2′, 3′ are ATR spectra for ZnO single crystal, placed in a uniform magnetic field with orientation $\vec{H} \perp \vec{k}$, $\vec{H} \| y$. The calculation was carried out for the sample ZO2-3 in the magnetic field of 100 kOe. The minima of experimental and calculated spectra correspond to the frequencies ν_{min} = 518 (1), 537 (2), 551 (3) cm^{-1} without any influence of the magnetic field on the sample and under the influence of the latter — ν_{min} = 518 (1′), 538 (2′), 552 (3′) cm^{-1}. The width of the spectra is Γ_s = 2, 3, 9 cm^{-1}.

Table 5 — The shift of the reflection spectrum minima and cyclotron frequency values of ZnO single crystal for some magnetic fields

H, kOe	$\nu_{min}(H) - \nu_{min}(H=0)$, cm^{-1}	$\Omega/2$, cm^{-1}
30	39	38
65	107	82
100	185	126

Table 6 — The distance between the plasma edges and cyclotron frequency values of ZnO single crystal placed in some magnetic fields

H, kOe	$[\nu_p(H) - \nu_p(H=0)]$, cm^{-1}	Ω, cm^{-1}
30	103	76
65	177	164
100	259	252

Table 7 — The areas of selective reflection of ZnO single crystals in some magnetic fields

H, kOe	30	65	100
ν, cm^{-1}	59...103	145...177	230...259

Fig. 15, *b*, shows ATR spectra of weakly doped zinc oxide ($n_0 = 6{,}6 \times 10^{17}$ cm^{-3}) without any influence of the magnetic field and the angle of the incidence in ATR prism of 30° (1, 1′), 35° (2, 2′), 50° (3, 3′). The space of the air gap between the sample ZO1-3 and ATR prism changed from 13 (1) to 3,4 (3) μm.

The minima spectra correspond to frequencies $\nu_{min} = 527$ (1), 550 (2), 563 (3) cm^{-1}.

The width of spectra is $\Gamma_s = 5$ (1), 17 (2), 28 (3) cm^{-1}. Curves 1′, 2′, 3′ were calculated under the influence of the uniform magnetic field of 100 kOe on zinc oxide single crystal (sample ZO1-3). The frequencies of the minima and width in ATR spectra are $\nu_{min} = 528$ (1′), 551 (2′), 564 (3′) cm^{-1}, $\Gamma_s = 7$ (1′), 19 (2′), 32 (3′) cm^{-1}. Points are experiment for ZnO single crystal (sample ZO1-3).

Fig. 15, *c*, shows the calculated ATR spectra of heavily doped ZnO ($n_0 = 2{,}0 \times 10^{18}$ cm^{-3}) (curves 1, 2, 3) with the angles of incidence of 30° (1, 1′), 35° (2, 2′), 50° (3, 3′) and with the space of the air gap between zinc oxide and ATR prism of 10,2 (1, 1′), 5,6 (2, 2′) and 2,6 (3, 3′) μm. Curves 1—3 are ATR spectra without any influence of a magnetic field on ZnO single crystal; curves 1′—3′are calculated ATR spectra in case of the influence of the uniform magnetic field of 100 kOe on ZnO single crystal (orientation $\vec{H} \perp \vec{k}$, $\vec{H} \| y$). The minima spectra correspond to the frequencies $\nu_{min} = 557$ (1′), 574 (2′), 582 (3′) cm^{-1}. The width of spectra is $\Gamma_n = 58$ (1′), 92 (2′), 99 (3′) cm^{-1}.

Fig. 15 (*a*—*c*) shows the shift of minima of ATR spectra to the area of high frequencies, with the increase of doping degree of ZnO single crystals, is observed. This means that SP attenuation coefficient also increases.

Fig 16, *a*, presents ATR spectra for undoped zinc oxide (sample ZO2-3) with the concentration of free charge carriers of $n_0 = 6{,}6 \cdot 10^{17}$ cm^{-3} and with the angle of incidence of *IR*-radiation in the ATR prism of 50°. The air gap between the ATR prism and ZnO single crystal is 4 μm. Scanning was carried out under the influence of the magnetic field of 0 (1), 30 (2), 65 (3) and 100 (4) kOe. The spectra minimum corresponds to the frequency $\nu_{min} = (551 \pm 1)$ cm^{-1} for all the values of the magnetic field. $\Gamma_s = 9$ cm^{-1} for curves 1—3 and 10 cm^{-1} for curve 4.

As it is presented in Fig. 16, *b*, the decrease of the ATR spectrum intensity is observed in the area of the manifestation of the minimum under the influence of the uniform magnetic field on ZnO sample.

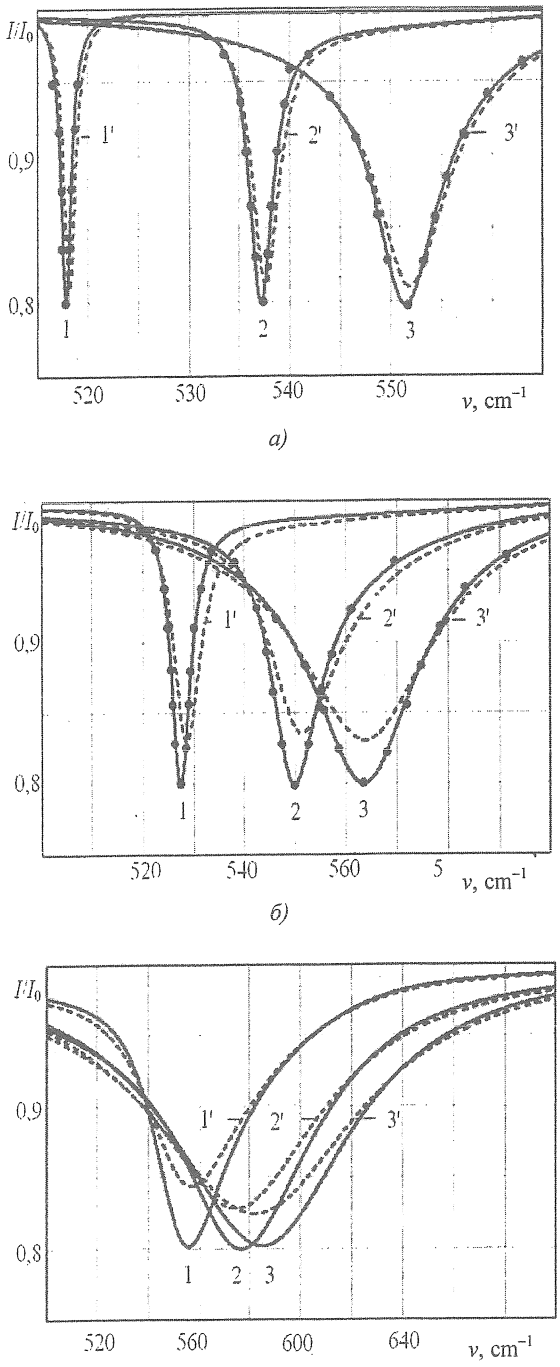

a — ZO2-3; *b* — ZO1-3; *c* — ZO6-B, 1—3 — $H = 0$ kOe; 1′—3′ — $H = 100$ kOe

Fig. 15 — ATR spectra of ZnO (curve — calculation; points — experiment)

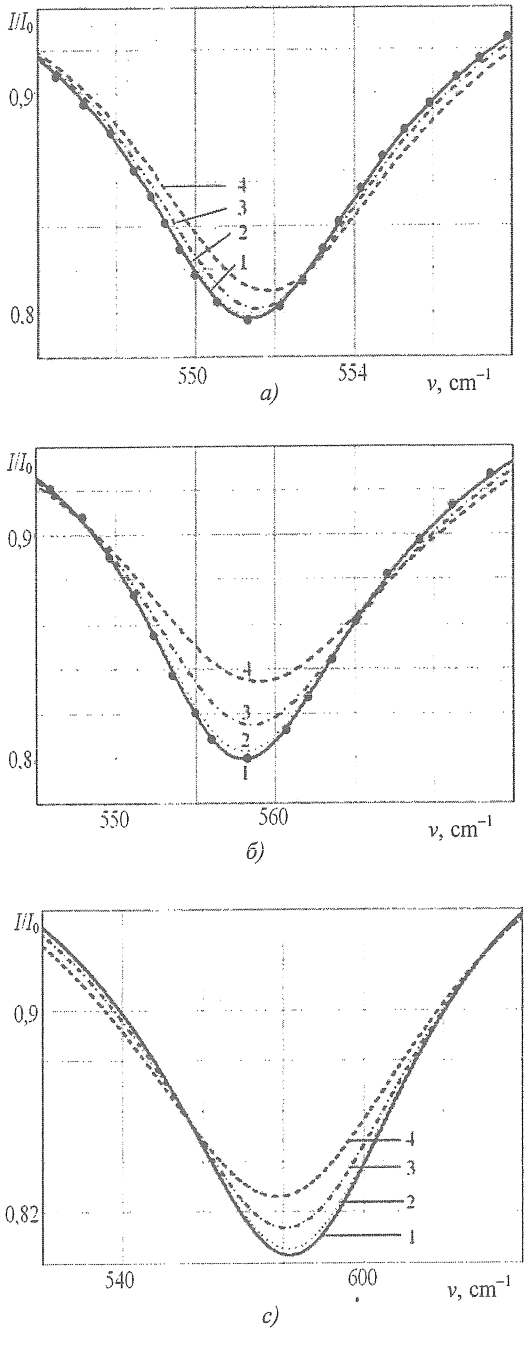

a — ZO2-3; *b* — ZO1-3; *c* — ZO6-B, 1—4 — $H = 0$; 30; 65; 100 kOe

Fig. 16 — ATR spectra of ZnO (curve — calculation; points — experiment)

Fig. 16, *b*, presents the influence of the magnetic field on the ATR spectra. The data from Tables 1 and 2 were used by the calculation for weakly doped sample ZO1-3 with the angle of incidence of 40° and with the air gap between the ATR prism and ZnO of 5 μm. The calculation was carried out under the influence of the magnetic field of 0 (1), 30 (2), 65 (3) and 100 (4) kOe respectively. Due to ATR spectra we can see that the increase of the magnetic field is accompanied by the increase of ATR spectra width, and therefore by

the increase of SP attenuation. The spectra minimum remains constant and corresponds to the frequency of SP $\nu_{min} = 558$ cm^{-1}. Γ_s for curves 1—4 is 20, 22, 25; 28 cm^{-1}.

The experimental spectrum (Fig. 16, *b*, point 1) was registered for weakly doped sample ZO1-3 at constant values of angle of incidence of *IR*-radiation in ATR prism ($\varphi = 40^0$) and air gap of 5 μm. The increase of the concentration of free charge carriers up to $2 \cdot 10^{18}$ cm^{-3} at constant value of uniform magnetic field of 30, 65 and 100 kOe, the angle of incidence and the gap between the prism and single crystal of 4 μm is followed by the shift of SP frequency to the low-frequency range of the spectrum (Fig. 16, *c*). The minima of spectra correspond to the frequencies $\nu_{min} = 581$ (1), 580 (2), 578 (3) cm^{-1} respectively and $\Gamma_s = 83$ (1, 2), 88 (3), 98 (4) cm^{-1}. Curve 1 was calculated without any influence of magnetic field on the single crystal.

We can see in Fig. 16, *a*, that the magnetic field, which influences the sample, manifests itself with the intensity of the coefficient I/I_0 in the minimum range of ATR spectrum at constant frequency of the minimum within the error of the experiment. With the increase of zinc oxide doping degree increases the influence of the magnetic field on the sample that is shown in ATR spectrum (Fig. 15, *b, c*).

The placement of the basic minima in ATR spectra changes a little with the increase of the magnetic field, they are slightly expanded. The analysis shows that they correspond to the surface modes ν^+ ν^- with $H \approx 0$ and pseudo-surface in stronger fields [36].

Let's assume that $K = q_x c/\omega$ is a combined wave vector. Fig. 17 presents the dispersion curves of ZnO single crystal for orientation $C\Pi y$, $\vec{k} \perp C$, $xy\Pi C$ obtained with the help of the method, described in [32], [33], [34], [35] in case of $H = 0$. The concentration of free charge carriers (electrons) in ZnO changed from $n_0 = 9{,}3 \cdot 10^{16}$ cm^{-3} (curves 1, 1′) up to $n_0 = 2{,}0 \cdot 10^{18}$ cm^{-3} (curves 3, 3′). Curves 2 and 2′ were registered with $n_0 = 6{,}6 \times \times 10^{17}$ cm^{-3}. Curves 1—3 correspond to high-frequency dispersion branches with the boundary frequency values of $\nu^+(k) = 561$ cm^{-1} (curve 1), 578 cm^{-1} (curve 2) and 627 cm^{-1} (curve 3); 1′—3′ are low-frequency dispersion branches with the boundary frequency values of $\nu^-(k) = 59$ cm^{-1} (curve 1′), 152 cm^{-1} (curve 2′) and 246 cm^{-1} (curve 3′). The points show the experimental values are obtained with the help of ATR method [3], [37], [38], [39]. Obtained from ATR spectra values of the limit frequency of SPPP (Surface Plasmon-Phonon Polaritons) (capital letters) $\nu^{\pm}$ coincide with the results [39].

Fig. 17 shows that the increase of the concentration of free charge carriers in ZnO (electrons) is followed by the shift of SPPP frequency to the high-frequency range of ATR spectrum, this characterizes the increase of

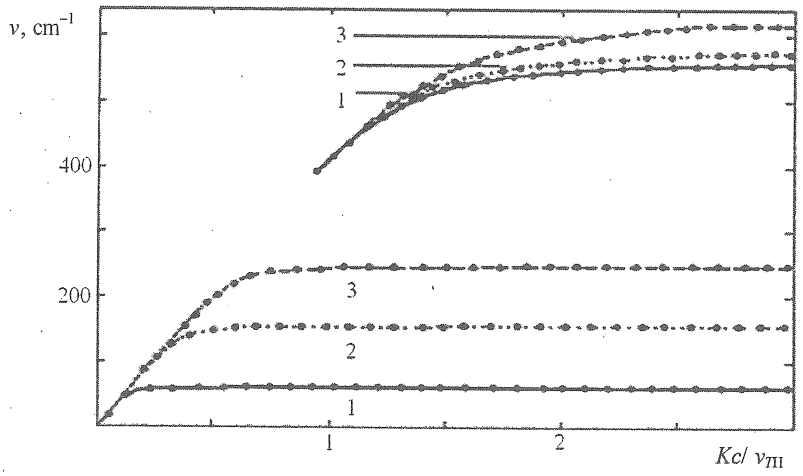

Fig. 17 — Dispersion curves of ZnO single crystal: *1* — ZO2-3; *2* — ZO1-3; *3* — ZO6-B (curve — calculation; points — experiment)

the attenuation coefficient of SP. SPPP high-frequency branches, regardless of the doping degree of the sample, begin with the frequency that corresponds to the ratio $\nu = \nu_{T\perp}$ and exists at $K >> 2\pi\nu/c$, asymptotically approaching the limit frequency of SP [3].

Fig. 18 presents the dispersion curves of weakly doped ZnO single crystal (sample ZO1-3) placed in the uniform magnetic field with the value from 0 up to 100 kOe for orientation $\vec{H} \perp \vec{k}$, $\vec{H}\parallel y$, $C\parallel y$, $\vec{k} \perp C$, $xy\parallel C$.

Fig. 18 (insert) shows that high-frequency dispersion curve does not change with the increase of the magnetic field from 0 to 100 kOe, whereas the lower dispersion branch shifts to the lower frequency range with the increase of the magnetic field.

Moreover, as follows from Fig. 18, the influence of the magnetic field on ZnO single crystal in the frequency range from 190 up to 350 cm^{-1} leads to the manifestation of another branch of the dispersion (limited by the value of the wave vector), which in case of the increase of external magnetic field from 30 kOe shifts to the high-frequency range and it is called "virtual" [36]. It is similar to the influence of the magnetic field on undoped and heavily doped ZnO single crystals (samples ZO2-3 and ZO6-B). The initial points for lower and upper dispersion branches correspond to the frequencies $\nu = 0$ and ν_T.

The asymptotes of "virtual" branch set equations are $1 + \varepsilon_1 \pm i\varepsilon_2 = 0$ [40].

Table 8 presents the boundary frequencies of plasmon-phonon and "virtual" dispersion branches for ZnO single crystals. For orientation $C\parallel x$, $\vec{k}\parallel C$, $xy\parallel C$, except high- and low-frequency dispersion branches, there exist one surface plasmon-phonon polariton branch, that manifests itself under the influence of the magnetic field on the sample and in the case of its absence. The boundary frequencies of which at different values of the magnetic field are presented in Table 9.

Fig. 19 presents manifestations of anisotropy of phonon and plasma subsystems of ZnO single crystal placed in the magnetic field of 30 kOe with direction $\vec{H} \perp \vec{k}$, $\vec{H}\parallel y$ which is detected by the number of dispersion curves. According to the orientation $C\parallel x$, $\vec{k}\parallel C$, $xy\parallel C$ (*see* Fig. 19, *a*) there exist 3 plasmon-phonon and 1 "virtual" dispersion curves. According to the orientation $C\parallel y$, $\vec{k} \perp C$, $xy\parallel C$ (*see* Fig. 19, *b*) and $C\parallel z$, $\vec{k} \perp C$, $xy \perp C$ (*see* Fig. 19, *c*) there are 2 plasmon-phonon branches respectively.

Fig. 20 shows the calculated dispersion curves of ZnO single crystal subjected to the influence of the magnetic field of 100 kOe. We can see, that in case of the increase of free charge carriers concentration and under the on fluence of a magnetic field, all three dispersion

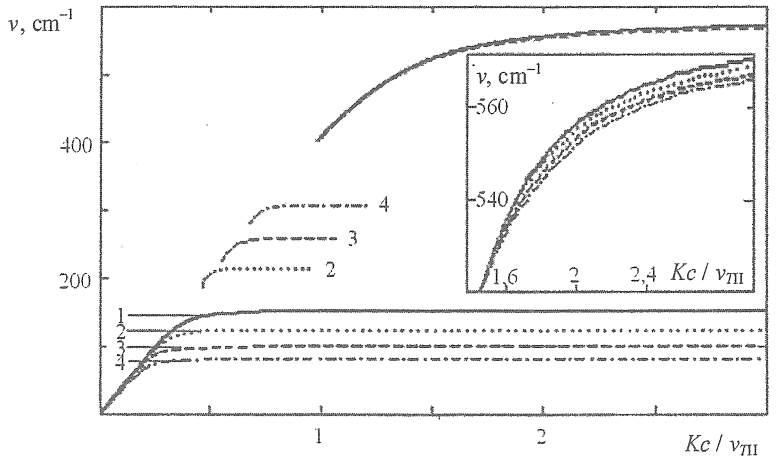

Fig. 18 — ZnO dispersion curves (sample ZO1-3) under the influence of the magnetic field: *1* — *4* — 0; 30; 65; 100 kOe

Table 8 — Boundary frequencies of various types of dispersion curves on ZnO subjected to the influence of a magnetic field

№	H, kOe	1		$30\cdot10^3$			$65\cdot10^3$			$100\cdot10^3$		
	Sample	ν^-_{pf}, cm^{-1}	ν^+_{pf}, cm^{-1}	ν^-_{pf}, cm^{-1}	ν_{ν_3}, cm^{-1}	ν^+_{pf}, cm^{-1}	ν^-_{pf}, cm^{-1}	ν_{ν_3}, cm^{-1}	ν^+_{pf}, cm^{-1}	ν^-_{pf}, cm^{-1}	ν_{ν_3}, cm^{-1}	ν^+_{pf}, cm^{-1}
$C\Pi x$, $\vec{k}\Pi C$, $xy\Pi C$												
1	ZO2-3	60	551	29	105	551	20	168	551	14	242	551
2	ZO1-3	151	570	58	138	570	87	231	571	76	281	571
3	ZO6-B	249	632	214	277	631	98	302	627	122	329	621
$C\Pi y$, $\vec{k} \perp C$, $xy\Pi C$												
1	ZO2-3	59	562	35	103	562	22	168	562	15	240	561
2	ZO1-3	152	579	128	190	579	102	237	580	83	288	580
3	ZO6-B	246	627	226	277	626	201	309	624	179	341	621
$C\Pi z$, $\vec{k} \perp C$, $xy \perp C$												
1	ZO2-3	60	551	29	104	551	20	168	551	14	242	551
2	ZO1-3	152	570	120	188	570	87	232	571	76	281	571
3	ZO6-B	110	632	130	336	631	84	340	627	122	348	621

Table 9 — Boundary frequencies of ZnO surface plasmon-phonon polariton branches subjected to the influence of a magnetic field

№	H, kOe	1	$30\cdot10^3$	$65\cdot10^3$	$100\cdot10^3$
	Sample	ν_{pf}, cm^{-1}	ν_{pf}, cm^{-1}	ν_{pf}, cm^{-1}	ν_{pf}, cm^{-1}
$C\Pi x$, $\vec{k}\Pi C$, $xy\Pi C$					
1	ZO2-3	69	77	151	239
2	ZO1-3	165	120	161	232
3	ZO6-B	266	248	248	274

branches shift to the high-frequency range, i. e. coefficient of attenuation of SP increases.

Thus, Figs. 18—20 present the calculated dispersion dependencies, which take the anisotropy of phonon and plasma subsystems in their harmonic approximation into account.

Let us consider another characteristic of SP-attenuation coefficient. Fig. 21 shows the frequency dependencies from the real $\nu(k')$ (solid line) and imaginary $\nu(k'')$ (dashed line) parts of the wave vector, taking into account the attenuation coefficient of phonon and plasmon subsystems of ZnO single crystal (sample ZO2-3, tables 1, 2). The curves, presented in Fig. 21, have characteristics similar to the obtained cation [41]. The recurvature (veer) back to the calculated dispersion relations appears as the layer is in antiphase with the wave that falls on wave that passed through the semiconductive layer and reflected from the boundary of this this layer, i. e. waves attenuate one another. This leads to the formation of the band gap and the recurvature appears on the dispersion curves.

For ZnO single crystals with different doping degrees the calculations $\Gamma_{sp}(\nu)$ were carried out without the influence of a magnetic field on the crystal (curves *1*—*3*, Fig. 22) and with the values of the magnetic field 30, 65 and 100 kOe (Fig. 22, curves *1'*—*3'*) with the ratio [3]:

$$\Gamma_{sp}(\nu)=\frac{\varepsilon_2(\varepsilon_0-\varepsilon_\infty)\nu^2\nu^2_{T\perp,\Pi}\gamma_f}{\varepsilon_\infty(\varepsilon_2+\varepsilon_\infty)\left(\left(\nu^+_{pf}\right)^2-\nu^2\right)^2+\varepsilon_2\left(\nu^+_{pf}\right)^2\nu^2_{T\perp,\Pi}}, \quad (2)$$

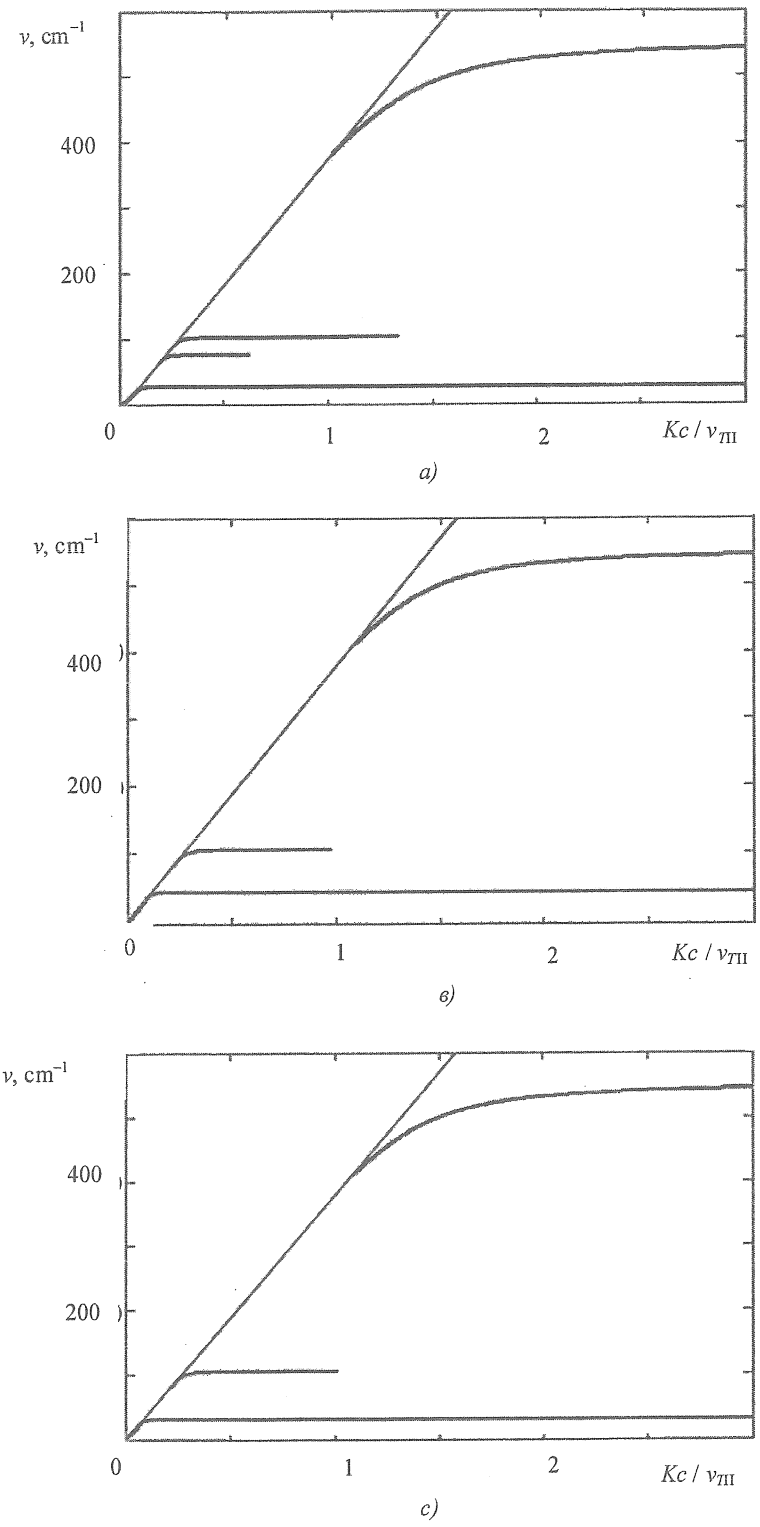

a — **C**$\vec{H}$**x**, $\vec{k}$‖*C*, *xy*‖*C*; *b* — **C**$\vec{H}$**y**, $\vec{k} \perp C$, *xy*‖*C*;
c — **C**$\vec{H}$**z**, $\vec{k} \perp C$, *xy* ⊥ *C*

Fig. 19 — Dispersion curves for ZnO single crystal in the magnetic field of 30 kOe with direction $\vec{H} \perp \vec{k}$, $\vec{H}$‖*y* and orientation

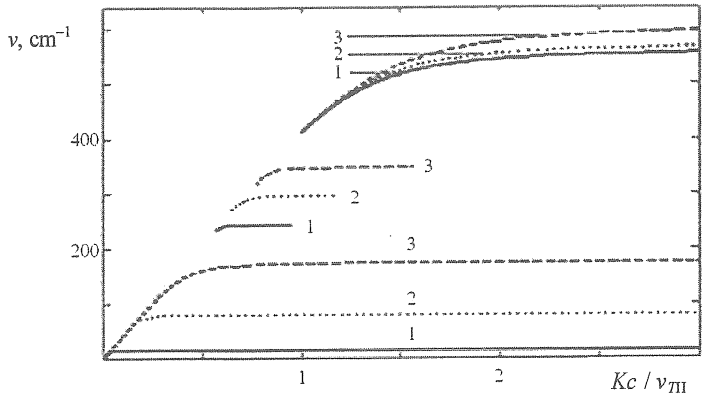

Fig. 20 — Different types of dispersion curves of ZnO single crystals in the magnetic field of 100 kOe, for orientation $C \parallel y$, $\vec{k} \perp C$, $xy \parallel C$: *1* — ZO2-3; *2* — ZO1-3; *3* — ZO6-B

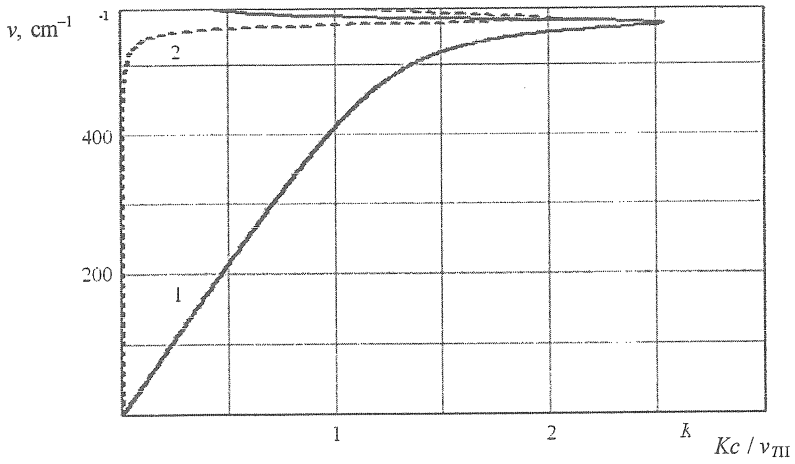

Fig. 21 — Dependencies $\nu\ (k')$ (curve *1*) and $\nu(k'')$ (curve *2*) for ZnO (sample ZO2-3), taking into account attenuation of phonons and plasmons

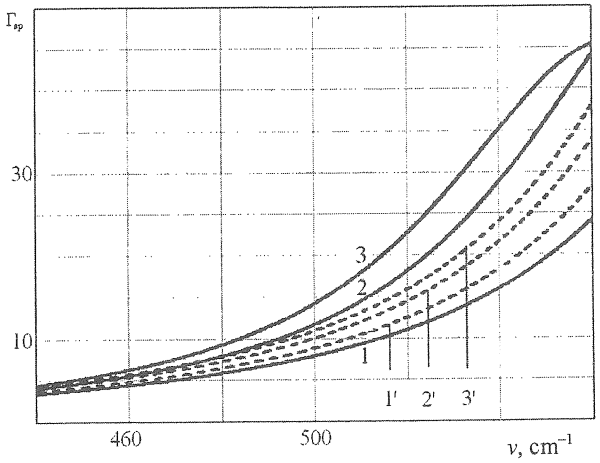

Fig. 22 — Dependence of SP attenuation coefficient from the frequency $\Gamma_{sp}(\nu)$ for ZnO single crystal: *1* — ZO2-3; *2* — ZO1-3; *3* — ZO6-B; *1'—3'* (sample ZO6-B) H = 30, 65, 100 kOe

where ν_{pf}^{+} is frequency limit of SP with $k \to \infty$; ε_2 is relative permittivity between the sample and the ATR element ($\varepsilon_2 = 1$).

Fig. 22 shows that with the increase of the concentration of free charge carriers in ZnO single crystals the attenuation coefficient of SP also increases. The similar pattern is observed in the case of increase of the magnetic field in which the investigated semiconductor is placed (the same result was obtained from analysis of the nature of dispersion curves in the magnetic field for samples of different doping degrees). Curves *1′—3′* (*see* Fig. 22) — $\Gamma_{sp}(\nu)$ for heavily doped sample ZO6-B subjected to the influence of the magnetic field on the crystal in the direction $\vec{H} \perp \vec{k}$, $\vec{H} \| y$ and with the values of the magnetic field of 30 (*1′*), 65 (*2′*), 100 (*3′*) kOe.

Table 10 presents Γ_s and Γ_{sp} data, obtained with the help of graphical method [32], [33],

Table 10 — Minimum width Γ_s in ATR spectrum and SP attenuation coefficient Γ_{sp} f ZnO with $\gamma_p \neq 0$, $\gamma_f \neq 0$ and $H = 0$ and 100 kOe

φ, °	H = 0 kOe				H = 100 kOe			
	ν_{min}, cm^{-1}	χ	Γ_s, cm^{-1}	Γ_{sp}, cm^{-1}	ν_{min}, cm^{-1}	χ	Γ_s, cm^{-1}	Γ_{sp}, cm^{-1}
$C \| x$, $\vec{k} \| C$, $xy \| C$								
ZO1-3 ($\gamma_{p\perp} = 280$ cm^{-1}, $\gamma_{p\|} = 260$ cm^{-1}, $\gamma_{f\perp,\|} = 13$ cm^{-1})								
30	511	1,528	21,49	12,40	513	1,55	32,97	21,31
35	536	1,780	100,18	73,53	538	1,84	224,88	157,10
50	552	2,120	310,73	248,91	552	2,21	—	504,57
ZO2-3 ($\gamma_{p\perp} = 150$ cm^{-1}, $\gamma_{p\|} = 170$ cm^{-1}, $\gamma_{f\perp,\|} = 11$ cm^{-1})								
30	500	1,473	7,78	4,78	500	1,474	8,82	4,80
35	522	1,677	14,39	11,75	522	1,68	14,93	11,90
50	538	1,972	80,15	69,86	538	1,985	83,89	72,31
$C \| y$, $\vec{k} \perp C$, $xy \| C$								
ZO1-3 ($\gamma_{p\perp} = 280$ cm^{-1}, $\gamma_{p\|} = 260$ cm^{-1}, $\gamma_{f\perp,\|} = 13$ cm^{-1})								
30	527	1,67	23,73	17,11	528	1,70	35,69	27,52
35	550	2,06	132,29	111,68	551	2,17	270,52	216,50
50	563	2,70	—	—	564	—	—	—
ZO2-3 ($\gamma_{p\perp} = 150$ cm^{-1}, $\gamma_{p\|} = 170$ cm^{-1}, $\gamma_{f\perp,\|} = 11$ cm^{-1})								
30	518	1,63	10,59	7,04	518	1,63	11,13	7,12
35	537	1,945	24,93	21,86	538	1,99	35,22	31,23
50	551	2,63	209,67	197,41	552	2,81	353,45	328,61
$C \| z$, $\vec{k} \perp C$, $xy \perp C$								
ZO1-3 ($\gamma_{p\perp} = 280$ cm^{-1}, $\gamma_{p\|} = 260$ cm^{-1}, $\gamma_{f\perp,\|} = 13$ cm^{-1})								
30	523	1,63	26,37	17,64	524	1,65	49,98	34,24
35	544	1,915	121,83	96,59	546	2,011	240,09	186,7
50	556	2,27	—	327,48	556	2,4	—	—
ZO2-3 ($\gamma_{p\perp} = 150$ cm^{-1}, $\gamma_{p\|} = 170$ cm^{-1}, $\gamma_{f\perp,\|} = 11$ cm^{-1})								
30	512	1,569	9,41	6,05	512,5	1,575	5,00	3,50
35	530	1,796	18,55	15,44	530	1,8	26,17	21,33
50	542	2,1	117,80	104,60	542	2,12	126,15	114,48

[34], for ZnO single crystals with different doping degrees, without the influence of magnetic field on the semiconductor and in case of its values 100 kOe and direction $\vec{H} \perp \vec{k}$, $\vec{H} \| y$. The angle of incidence in the ATR prism is 30°; 35° and 50°.

It is shown in Table 10 that, with the increase of the angle of incidence and concentration of free charge carriers in ZnO single crystals the SP-attenuation coefficient also increases. It is similar is to influence of plasmon-phonon attenuation and the external magnetic field on Γ_s and Γ_{sp} of ZnO single crystal.

Conclusions. Thus, using the non-destructive methods of *IR*-spectroscopy, we conducted the investigation of the dependence of optical and electorphysical (electrophysical) characteristics of optically-anisotropic semiconductors from the influence of a uniform magnetic field on them while studying ZnO single crystal (Faraday and Voigt configurations). For the first time the areas with new oscillations (caused by the influence of a uniform magnetic field) were found in the *IR*-reflection spectra of ZnO single crystal as well as plasmon-phonon interaction was studied under the above conditions. The influence of the magnetic field on the basic properties of surface polaritons for three mutually orthogonal orientations of the optical axis and the wave vector was established.

It is shown that the influence of the magnetic field on ZnO single crystal causes anisotropy and the shift of the intervals $R(\nu)$ in the range of maximum values to the high-frequency range of the spectrum. This allows along with commonly used optically-mechanical modulators, whose work is based on the optical anisotropy of reflection coefficients for different orientations of electric vector and optical axis of the crystal, to create magneto-optical modulators and to determine the concentration and mobility of free charge carriers and so on.

References

1. *Kuzmina.* Zinc oxide. Receipt and optical properties / Kuzmina, Nikitenko. — Moscow. — Nauka, 1984. — P. 168 (in Russian).
2. Microelectronic Magnetic Field Sensor Facilities / Bolshakova [et al.]. — Lviv : Lvivs'ka Politekhnika, 2001. — P. 412 (in Ukrainian).
3. *Venger.* Residual Rays Spectroscopy / Venger, Melnichuk, Pasichnyk. — Kyiv : Naukova Dumka, 2001. — P. 192 (in Ukrainian).
4. *Rodnyi.* Optical and Luminescent Properties of Zinc Oxide (review) / Rodnyi, Khodyuk // Optyka, Spektroskopiya. — 2011. — Vol. 111, № 5. — P. 814—824 (in Russian).
5. Infrared dielectric function and phonon modes of high-quality ZnO films / N. Ashkenov [et al.] // Journal of applied physics. — 2003. — Vol. 93, № 1. — P. 126—133.
6. UV Detectors based on ZnO Nanocrystalline Films / Kryvchenko [et al.] // Technical Physics Journal. — 2008. — Vol. 78, issue 8. — P. 107—111 (in Russian).
7. Polarized photoreflectance spectra of excitonic polaritons in a ZnO single crystal / S. F. Chichibu [et al.] // Journal of applied physics. — 2003. — Vol. 93, № 1. — P. 756—758.
8. *Sharma, P.* Analysis of ultraviolet photoconductivity in ZnO films prepared by unbalanced magnetron sputtering / P. Sharma, K. Sreenivas, K. V. Rao // Journal of applied physics. — 2003. — Vol. 93, № 7. — P. 3963—3970.
9. Zinc oxide as an ozone sensor / R. Martins [and oth.] // Journal of applied physics. — 2004. — Vol. 96, № 3. — P. 1398—1407.
10. Modification of Physical Properties of Wide Band-gap Semiconductors $A^{II}B^{VI}$ / Zagoruiko [et al.]. — Institute of Single Crystals, Khar'kov, 2005. — P. 350 (in Russian).
11. *Venger, E. F.* Anisotropy of ZnO single crystal reflectivity in the area of residual rays / E. F. Venger, A. V. Melnichuk, L. Yu. Melnichuk // Phys. Status solidi (b). — 1995. — Vol. 188, № 2. — P. 823—831.
12. Growth of ZnO Nanocrystals by pulse laser deposition on sapphire and silicon and the IR-spectra of the nanocrystals / Bazhenov [et al.] // Semiconductors, 2009. — Vol. 43, № 11. — P. 1532—1538.
13. *Melnichuk, A. V.* Anisotropy of electrical propreties of ZnO single crystals / A. V. Melnichuk, L. Yu. Melnichuk, Yu. A. Pasechnik // Fiz. Tverd. Tela. — 1994. — Vol. 36, issue 9. — P. 2624—2633 (in Russian).
14. *Golovin Yu. I.* Magnetoplasticity of Solids. (review) / Yu. I. Golovin // Fiz. Tverd. Tela. — 2004. — Vol. 46, issue 5. — P. 769—803 (in Russian).
15. *Buchachenko, A. L.* Effect of magnetic field on mechanics of nonmagnetic crystals : The nature of magnetoplasticity / A. L. Buchachenko // Journal of Experimental and Theoretical Physics. — 2006. — Vol. 129, issue 5. — P. 909—913.
16. *Darinskii, B. M.* Spin effects in nonmagnetic crystals in a magnetic field / B. M. Darinskii,

V. N. Feklin // Physics of the Solid State. — 2006. — Vol. 48, issue 9. — P. 1614—1616.

17. *Moss, T. S.* Semiconductor opto-electronics / T. S. Moss, G. J. Burrel, B. Ellis. — Moscow : Mir, 1976. — P. 431 (in Russian).

18. *Baer, W. S.* Faraday Rotation in ZnO Determination of the Electron Effective Mass / W. S. Baer // Phys. Rev. — 1967. — Vol. 154. — P. 785—789.

19. Molecular nitrogen (N) acceprors and isolated nitrogen (N) acceptors in ZnO crystals / N. Y. Garces [et al.] // Journal of applied physics. — 2003. — Vol. 94, № 1. — P. 519—524.

20. A Comprehensive review of ZnO Materials and devices / Ü. Özgür [et al.] // Journal of applied physics. — 2005. — Vol. 98. — P. 041301.

21. Electrical conductivity and magnetic properties of thin ZnO films doped with cobalt / V. G. Kytin [and oth.] // Physics of the Solid State. — 2010. — Vol. 44, issue 2. — P. 164—169.

22. Influence of plasmon-phonon coupling on the reflection coefficient in ZnO uniaxial polar semiconductor / E. F. Venger [et al.] // Ukrainian Physical Journal. — 2000. — Vol. 45, № 8. — P. 976—984 (in Ukrainian).

23. The use of a strong uniform magnetic field to study ZnO single crystals / E. F. Venger [et al.] // Fiz.-Math. Zapysky. Zb. nauk. pr. — Nizhyn : M. Gogol NSU, 2007. — P. 5—11 (in Ukrainian).

24. Investigation of ZnO single crystals subjected to high uniform magnetic field in IR spectral range / E. F Venger [et al.] // Semiconductor Physics, Quantum Electronics & Optoelectronics. — 2008. — Vol. 11, № 1. — P. 6—10.

25. IR-spectroscopy investigations of ZnO and 6H-SiC single crystals / E. F Venger [et al.] // Sb. nauchn. tr. (Georgia, Telavi State Univ.). — 2008. — №2 (24). — P. 30—34 (in Russian).

26. *Tsydilkovs'kyi, I. M.* Electrons and holes in semiconductors / I. M. Tsydilkovs'kyi. — Moscow : Nauka, 1972. — P. 640 (in Russian).

27. *Tsydilkovs'kyi, I. M.* The band structure of semiconductors / I. M. Tsydilkovs'kyi. — Moscow : Nauka, 1978. — P. 328 (in Russian).

28. Magneto-refractive effect in ZnO and 6H-SiC single crystals / E. F Venger [et al.] // Optoelektronika i Poluprovodnikovaya Tekhnika. — 2008. — Issue 43. — P. 30—37 (in Ukrainian).

29. Specific features of the reflection of IR-radiation by crystalline dielectrics in a magnetic field / A. F. Kravets [et al.] // JETP. — 2004. — Vol. 126, № 6. — P. 1362—1366 (in Russian).

30. Optical and magneto-optical properties and magneto refractive effect in metal-insulator CoFe-Al_2O_3 granular films / V.G. Kravets [et al.] // J. Appl. Phys. — 2005. — Vol. 98, № 4 — P. 043705 (7 pages).

31. *Voytsekhovskyi, A. V.* Semiconductor Optics: Training manual / A. V. Voytsekhovskyi, A. S. Petrov, G. I. Potakhova. — Tomsk : Tomsk Univ., 1987. — P. 222 (in Russian).

32. Investigation of surface polaritons in a strong uniform magnetic field / E. F Venger [et al.] // Fiz.-Math. Zapysky : zb. nauk. pr. — Nizhyn : M. Gogol NSU, 2009. — P. 50—64 (in Ukrainian).

33. Effect of strong magnetic field on surface polaritons in ZnO / E. F. Venger [et al.] // Semiconductor Physics, Quantum Electronics & Optoelectronics. — 2010. — Vol. 13, № 2. — P. 16—22.

34. ATR-method in surface polariton spectroscopy / G. A. Puchkovskaya [et al.] // Ukrainian Physical Journal. — 1980. — Vol. 25, № 2. — P. 271—276 (in Russian).

35. Surface Polaritons in Semiconductors and Dielectrics / N. L. Dmitruk [et al.]. — Kiev : Nauk. Dumka, 1989. — P. 375 (in Russian).

36. *Agranovich, V. M.* Surface Polaritons / V. M. Agranovich, D. L. Mills. — Moscow : Nauka, 1985. — P. 525 (in Russian).

37. *Melnichuk, A. V.* Attenuation of ZnO surface plasmon-phonon polaritons / A. V. Melnichuk, Yu. A. Pasechnik // Physics of the Solid State. — 1996. — Vol. 38, № 8. — P. 2343—2346 (in Russian).

38. *Melnichuk, A. V.* Effect of anisotropy on the dispersion dependencies of ZnO surface plasmon-phonon polaritons / A.V. Melnichuk, L. Yu. Melnichuk, Yu. A. Pasechnik // Physics of the Solid State. — 1996. — Vol. 38, № 2. — P. 651—653 (in Russian).

39. *Melnichuk, A. V.* Surface plasmon-phonon polaritons in hexagonal zinc oxide / A. V. Melnichuk, L. Yu. Melnichuk , Yu. A. Pasechnik // Technical Physics Journal. — 1998. — Vol. 68, issue 1. — P. 58—62 (in Russian).

40. Surface magnetoplasmon-optic phonon modes in InSb / E. D. Palik [et al.] // Phys. Lett., A. — 1973. — Vol. 45 A, № 2. — P. 143—144.

41. *Shramkova, O. V.* Attenuation of electromagnetic waves in a semiconductor superlattice placed in a magnetic field / O. V. Shramkova // Technical Physics Journal. — 2004. — Vol. 74, issue 2. — P. 92—97 (in Russian).

Материал поступил в редакцию 06.04.2012 г.

С помощью спектроскопии отражения внешнего (EF) и нарушенного полного внутреннего отражения (ATR) исследование оптических и электрофизических свойств полярного одноосного оптически анизотропного монокристалла ZnO, помещённого в однородное магнитное поле (Фарадея и Фойгт-конфигурации), не проводилось. Область отображения новых колебаний, вызванных воздействием однородного магнитного поля, было обнаружено впервые в спектрах внешнего ИК-отражения монокристалла ZnO. Взаимодействие фононов и плазмонов исследовали при тех же условиях. Влияния магнитного поля на основные свойства поверхностных поляритонов (SP) в соответствии с ориентациями выявлено не было.